Supporting Information

Intrinsic anionic rearrangement by extrinsic control: Transition of RS and CRS in thermally elevated TiN/HfO_2/Pt RRAM

Writam Banerjee[*a,b], Wu Fa Cai*[a,b], Xiaolong Zhao*[a,b], Qi Liu*[a,b], Hangbing Lv*[a,b], Shibing Long*[a,b] and Ming Liu*[a,b]*

Keywords: resistive random access memory (RRAM); crossbar; resistive switching (RS); complementary resistive switching (CRS); nonlinearity

Figure S1: The SET compliance dependent behaviors.

Figure S2: Effect of RESET voltage on CRS.

Figure S3: Device-to-device performance analysis.

Figure S4: The cycle-to-cycle CRS switching degradation at 85^{o}C.

Figure S5: Thermal effect on HRS.

Video file S6: The real-time measurement video of the CRS at 30^{o}C.

Video file S7: The real-time measurement video of the CRS at 100^{o}C.

Table S8: Comparison with the reported results.

[a]*Key Laboratory of Microelectronic Devices & Integrated Technology, Institute of Microelectronics, Chinese Academy of Sciences, No. 3 BeiTuCheng West Road, ChaoYang District, Beijing 100029, China.*
[b]*Jiangsu National Synergetic Innovation Center for Advanced Materials (SICAM), Nanjing 210009, China.*
**E-mail: writam.banerjee@gmail.com, writam.banerjee@ime.ac.cn*
Tel: 86-10-82995582; Fax: 86-10-82995583

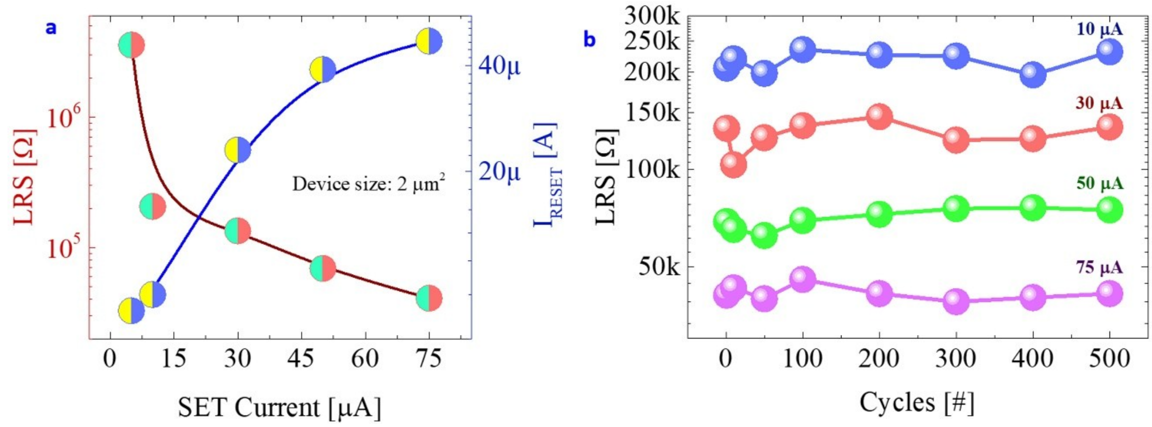

Figure S1: The SET compliance dependent behaviors. (a) The LRS is following an increasing and the IRESET is following a decreasing trend with the decreasing I_{CC}. **(b)** The different levels are showing good stability over switching cycles.

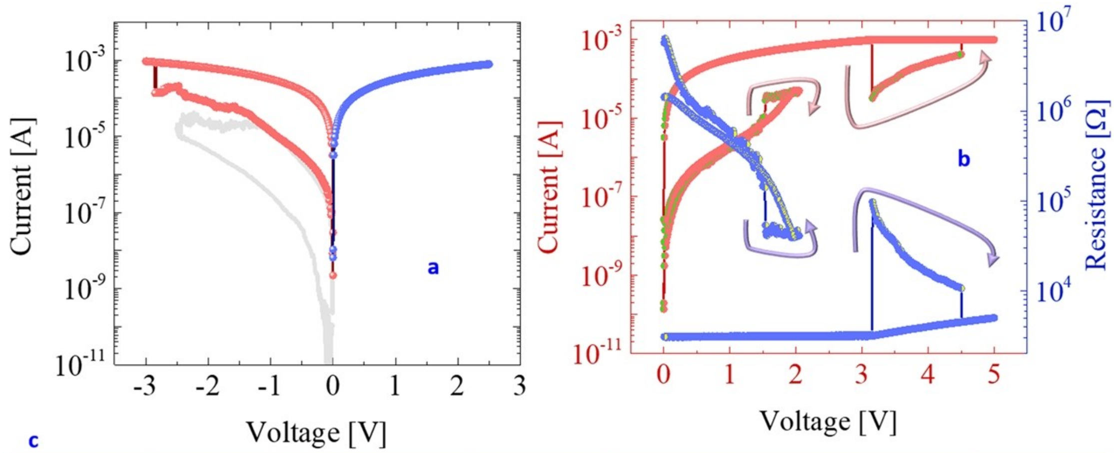

c

Type	*-V*	*Procedure*	*Current*	*CRS: I-V switching direction*	*Status*
1	RESET	Voltage controlled	50 µA	Clockwise switching: HRS → LRS → HRS	Controllable
2	SET	RESET failure	> 1 mA	Anti-clockwise switching: LRS → HRS → LRS	Stuck to LRS

Figure S2: Effect of RESET voltage on CRS. (a) After the 2nd forming process, if the device is operated higher than -2.5 V, then instead of resetting the device another SET switching in negative voltage is observed. In this situation the nano-filament growth direction is reverse way than the normal positive bias SET. **(b)** A reverse CRS process is achieved with a positive bias due to the RESET failure with negative bias. **(c)** Unfortunately, the reverse CRS is not stable and is prone to stuck to the LRS.

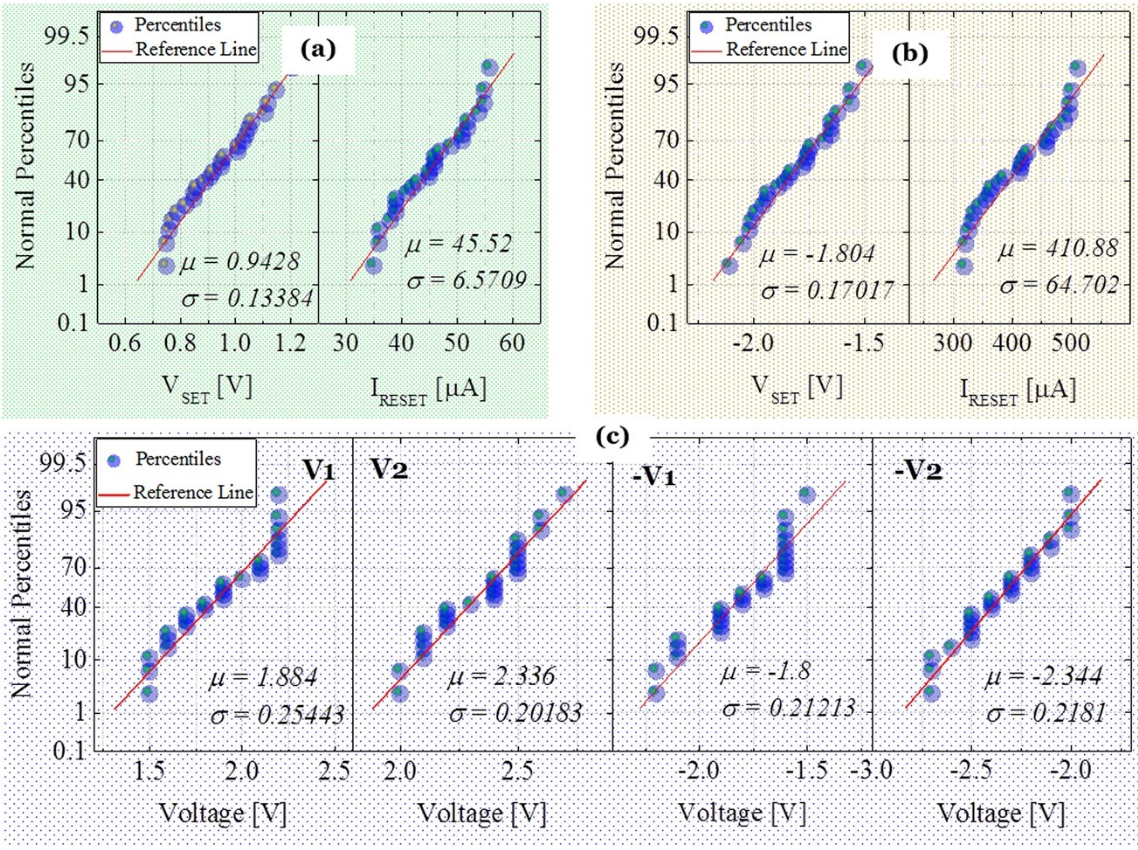

Figure S3: Device-to-device performance analysis. The device-to-device variation of the V_{SET} and I_{RESET} for the (a) 1st-RS mode and (b) 2nd-RS mode. Both the V_{SET} and I_{RESET} is higher for the 2nd-RS as compare to the 1st-RS. In addition, the V_{SET} is indicating different polarity in-between 1st and 2nd RS modes. (c) The OFF to ON and ON to OFF transition voltage variation for the CRS mode. Here, V1 is the change from the OFF state to ON state in the positive bias, V2 is the change from the ON state to OFF state in the positive bias, -V1 is the change from the OFF state to ON state in the negative bias, and -V2 is the change from the ON state to OFF state in the negative bias.

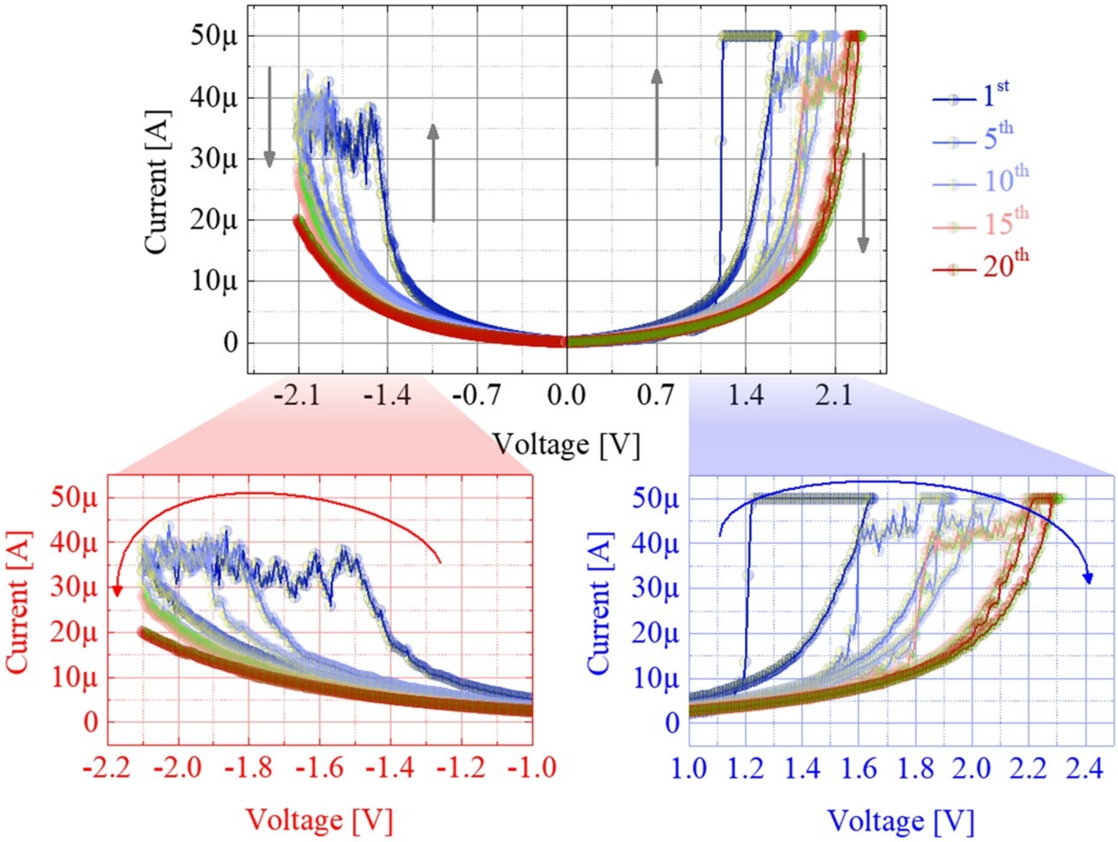

Figure S4: The cycle-to-cycle CRS switching degradation at 85°C. The high temperature CRS process is not so stable like room temperature.

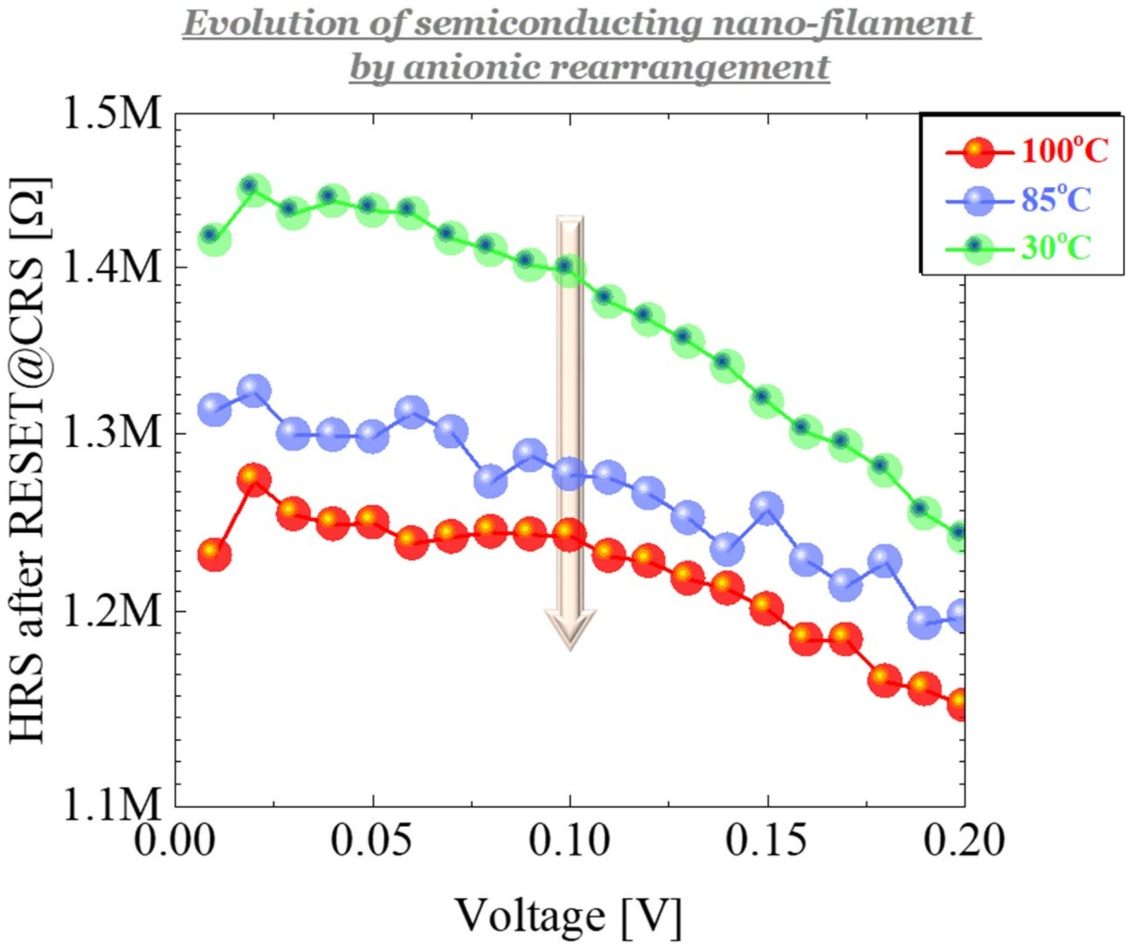

Figure S5: Thermal effect on HRS. The temperature dependent HRS is showing a non-metallic filament formation in the TiN/HfO_2/Pt X-point devices.

Supplementary video files S6: The real-time measurement video of the CRS phenomena at 30°C in the HfO_2-based X-point.

Supplementary video files S7: The real-time measurement video of the CRS phenomena at high temperature of 100°C, in the HfO_2-based X-point.

Supplementary Table S8:

Table S7: The comparison of the reported results of the RRAM devices operated with CRS mode.

Ref.	Structure	Stack	Extra electrode	Forming	Complementary Resistive Switching Parameters			
					I_{CC} [mA]	Read ΔV [V]	Storage ΔV [V]	T [°C]
→ ***This work***	***X-point***	***Pt/HfO2/TiN/Pt***	***No***	***+2.5 V @ 10 µA***	***0.01 – 0.5***	***0.5 - 1.5***	***1.0 - 4.0***	***RT - 150***
Wouters et al. [20]	1R	TiN/HfO2/Hf/HfO2/TiN	Hf	--	3.0	0.8	1.1	RT
Ambrogio et al. [21]	1R	TiN/HfO2/TiN/HfO2/TiN	TiN	+1 V @ 500 µA	0.5	0.5	1.0	RT
Soni et al. [19]	1R	Pt/SiOx/Ge0.3Se0.7/Cu/Ge0.3Se0.7/SiOx/Pt	Cu	+0.2 V @ 100 µA	1.0	0.2	0.3	RT
Linn et al. [11]	1R	Pt/solid electrolyte/Cu/solid electrolyte/Pt	Cu	--	0.8	0.7	1.0	RT
Tseng et al. [32]	1R	TiN/ZnO/SiOx/ZnO/Pt	No	+9 V @ 1 mA	20	0.7	1.5	RT
Yang et al. [27]	X-point	Pd/TaOy/Ta2O5-x/Pd	No	-4 V	1.5	1.5	2.0	RT
Wang et al. [12]	X-point	Ti/TiOx/Cu/TiOx/Ti	Cu	+3 V @ 1 mA	0.7	0.3	1.0	RT
Nardi et al. [24]	1R	TiN/HfOx/TiN	No	--	3.0	0.7	1.0	RT
Banerjee et al. [35]	3D VRRAM	TiN/TiOx/Al2O3/IrOx	No	+10 V@ 100 µA	0.09	0.5	9.0	RT
Lee et al. [16]	1R	Pt/ZrOx/HfOx/TiN/ZrOx/HfOx/Pt	TiN	+2V @ 1 mA	0.5	0.5	1.0	RT
Chen et al. [14]	1R	Pt/AlN/TiN/AlN/TiN/Pt	TiN	--	1.0	1.5	3.0	RT
Zhang et al. [26]	1R	TiN/HfOx/TiN	No	--	5.0	0.4	1.0	RT
Jana et al. [29]	1R	TiN/Al2O3/GdOx/IrOx	No	-3 V @ 1 mA	1.0	1.0	4.0	RT
Rosezin et al. [15]	1R	Pt/SiO2/Cu/Pt/Cu/SiO2/Ti/Pt	Cu/Pt/Cu	--	14.0	2.0	4.0	RT
Lee et al. [13]	1R	Pt/Ta2O5-x/Ta/Ta2O5-x/Pt	Ta	+4 V @ 10 mA	20.0	1.0	2.0	RT
Chai et al. [34]	1R	Ag/amorphous-carbon/CNT/Ag	No	--	0.08	5.0	10.0	RT
Zhang et al. [30]	1R	TiN/Al2O3/HfOx/TiN	No	+0.6 V @ 100 µA	0.1	0.3	1.4	RT
Bae et al. [33]	1R	Pt/TiOx/TiOxNy/TiOx/Pt	TiOxNy	-10 V @ 10 µA	0.1	0.5	1.0 – 3.0	RT
Tang et al. [31]	1R	TiN/TiNxOy/TiO2-x/Pt	No	-2 V	10.0	0.2	1.2	RT
Lin et al. [17]	1R	Pt/ZnO/ZnWOx/W/ZnWOx/ZnO/Pt	W	--	10.0	0.5	2.0	RT
Schmelzer et al. [23]	1R	Ta/TaOx/Pt	No	--	4.0	2.0	4.0	RT
R: resistor; 2D: two-dimensional; 3D: three-dimensional; X: cross; I_{CC}: current compliance; T: temperature; RT: room temperature								